Available online at www.sciencedirect.com
ScienceDirect
Journal of the European Ceramic Society 28 (2008) 2791–2800
www.elsevier.com/locate/jeurceramsoc

Multilayer SiC for thermal protection system of space vehicles: Manufacturing and testing under simulated re-entry conditions

S. Biamino [a,*], V. Liedtke [b], C. Badini [a], G. Euchberger [b], I. Huertas Olivares [b], M. Pavese [a], P. Fino [a]

[a] *Dipartimento di Scienza dei Materiali e Ingegneria Chimica, Politecnico di Torino, Corso Duca degli Abruzzi 24, 10129 Torino, Italy*
[b] *Austrian Research Centers GmbH, A-2444 Seibersdorf, Austria*

Received 16 June 2007; received in revised form 27 March 2008; accepted 4 April 2008
Available online 3 June 2008

Abstract

Two types of laminated multilayer silicon carbide plates were processed by tape casting, de-binding and pressureless sintering. The specimens were subject to thermal re-entry testing under conditions as derived from the HERMES study: up to 100 combined thermal and air pressure cycles were performed. After the first cycle, all samples lost about 1.5% of their initial mass. This was caused by burn-off of the carbon added as sintering aid or left after thermal decomposition of binder and plasticizer used in the tape casting process. During subsequent thermal cycles, all samples slightly gained mass due to formation of silica on the surface and partial oxidation at the core. After completing 100 cycles, microstructure and mechanical behaviour of specimens were compared to that of the as-processed material. A flexural strength higher than 100 MPa and a Young modulus of about 130 GPa were retained by all the specimens.

Keywords: Tape casting; Sintering; SiC; Mechanical properties; Re-entry test

1. Introduction

Future spacecraft are likely to be equipped with re-usable components or may be designed as fully re-usable vehicles. The first approach may be pursued for launch vehicles, e.g. as already outlined in the European Reusable Launch Vehicles study, and it is likely to be applied for the next generation heavy launchers that will finally replace the Ariane 5 versions currently in use.

Fully reusable manned spacecraft will comprise of a completely different technology base than the currently still used, but soon being outphased US Space Shuttle. The Space Shuttle is built of a metallic fuselage and wing structure, covered with ceramic tiles as thermal protection for surviving the re-entry into Earth's atmosphere. The technology employed may be regarded as state-of-the-art of the late 1960s and early 1970s, despite all attempts for refurbishment and improvements in the aftermath of the Columbia disaster in 2003.[1] Recent incidents during the STS-122 mission indicate that the fundamental problem of the impact-sensitive heat shield has not been fixed, and it is unlikely that the thermal protection system can be modified in such a way that it will meet the standards of heat shield technology available today.

Recent technology studies and flight vehicles (both still in progress or already completed) will most likely be based on thermal protection systems that double as structural components. For parts with moderate thermal loads, e.g. vehicle upper side and most parts of the fuselage, metallic thermal protection system (TPS) panels are favourable because of their rather affordable price, their ease of machining and their good strain-to-failure. Suitable materials may be oxide dispersion strengthened (ODS) alloys such as PM1000 or PM2000, despite the fact that the only supplier has stopped production. Alternatively, commonly used nickel-based superalloys could be employed.

For temperatures exceeding 800–1000 °C, as appearing at the leading edges, the nose cap, the chin panel, and the control surfaces, ceramic materials are mandatory. Monolithic ceramics would face the same brittleness and lack of impact tolerance as the Space Shuttle tiles, therefore reinforced ceramic materials are being favoured. When high strength is required, carbon fibre reinforced silicon carbide, commonly known as C_f/SiC, is

* Corresponding author. Tel.: +39 011 5644674/99; fax: +39 011 5644674/99.
E-mail address: sara.biamino@polito.it (S. Biamino).

0955-2219/$ – see front matter © 2008 Elsevier Ltd. All rights reserved.
doi:10.1016/j.jeurceramsoc.2008.04.006

the material of choice because of its excellent strength at high temperatures, the low specific weight, the impact and damage tolerance, and the mature production technology.[2] For moderate mechanical loads, more cost-efficient short fibre reinforced (even if nowadays the employment of short fibres for composite preparation is not completely approved because of the problems with health protection that such type of material brings) or advanced monolithic ceramics could also be considered.

Based on preliminary design studies of the EXPERT programme, reusable ceramic plates for the additional thermal protection of critical parts of metallic TPS panels may be required. Additional ceramic protection against oxidation is also required for Cf/SiC composite. Novel ceramic films could be a promising technical solution, provided that such materials can be manufactured, bonded to a metallic substructure, and qualified in an appropriate way.

Therefore, novel ceramic thermal protection concepts are a real need for the space industry, and SiC blankets are prime candidates to meet these requirements.

Generally speaking SiC shows potential for such an application owing to its peculiar properties: thermal stability at very high temperature, low density, high stiffness and fairly good strength, high hardness and erosion resistance, self passivating behaviour in oxidising environment. However, SiC presents some lacks that ought to be overcome: rather poor toughness; poor insulation capability at room temperature, but greatly increasing with temperature increase[3]; active oxidation at high temperature and under low partial pressure of oxygen.[4,5] Since 1992 Clegg showed as SiC-based laminates can display improved toughness with respect to conventional SiC[6] providing that weak interfacial bonds between the layers form. The weakness of interfacial bonds as well as residual stresses are believed to promote crack deflection phenomena, which result in the increase of the work of fracture. The integration within the SiC-based laminates (as well as in the architecture of other ceramic laminates) of secondary phases, interlayers with modified composition and porous layers was exploited for increasing toughness.[7–10]

The current paper describes the manufacturing process and results of the characterisation work on a laminated silicon carbide material, processed by tape-casting, de-binding and sintering, that has been submitted to thermal re-entry testing under test conditions representing the trajectory of the HERMES vehicle.[11]

2. Experimental

2.1. Material processing

Multilayer SiC specimens have been prepared at Politecnico di Torino according to a processing path involving several steps: preparation of a slurry, tape-casting, solvent evaporation, stacking green tapes to obtain a laminate, de-binding and sintering. Two kinds of specimens have been prepared: the first one showing only dense layers after sintering and the second one integrating porous layers in the multilayer architecture. In order to process the laminate of the first type, the slurry has been prepared by dispersing SiC ceramic powder (H.C. Starck, mean particle size 0.55 μm), carbon (Alfa Aesar, flake 7–10 μm) and boron (H.C. Starck, amorphous grade I) powders used as sintering aids, in a mixture of organic solvents containing a proper dispersant (fish oil). Mixing was carried out for 12 h in an alumina jar and using alumina milling balls. Afterwards a plasticizer (polyethylenglycole, Bisoflex 102 Cognis) and a binder (polyvinilbutyral, Butvar B76 Solutia) were added to the slurry and the mixing process was further prolonged for about 24 h. The composition of the slurry is shown in Table 1. This slurry was submitted to tape-casting, thus a green layer was deposed on a moveable plastic support (Mylar film). The doctor blade gap of 1 mm and the support speed of 100 mm/min were adopted according the process developed in a previous work.[12] Solvents were removed by controlled evaporation in air; this slow process, lasting about 12 h, allowed to obtain defect-free SiC green layers about 200–250 μm thick with the composition also reported in Table 1. The green tapes were cut, thus obtaining sheets suitable for the preparation of the multilayer specimens; the sheets were stacked in the multilayer structure made of ten layers. The surface of the layers was painted by using a solution made of water, ethanol and polyvinyl alcohol in order to improve adhesion between the layers, the smooth side of one layer facing the rough side of the subsequent one.

The specimens containing porous layers were obtained by integrating in the laminate architecture SiC layers processed by tape-casting of a slurry, as usual, but containing a sacrificial material suitable for providing residual porosity after sintering. To this purpose starch (Sigma–Aldrich) was added as pore-forming agent to the slurry, whose composition is shown in Table 1. The SiC tapes (resulting in dense layer after sintering) and the starch-containing tapes (giving rise to porous layers) were stacked according to the following sequence: d_3, p, d_2, p, d_3 (where d = SiC tape; p = tape containing starch). The adhesion between the layers was attained by painting a gluing solution made of water, ethanol and polyvinyl alcohol (PVA) before stacking next layer and rolling with a mandrel in order to let the successive layer adhere without the formation of air inclusions.[12]

De-binding treatment was carried out under argon atmosphere up to 800 °C and resulted in the thermal decomposition of binder, plasticizer, PVA coming from the gluing solution and starch (if present). Flat specimens of multilayer SiC were put in between graphite plates during this treatment. The organic components left carbonaceous residual species after decomposition. In the case of the multilayer not containing starch (but SiC only) it was assessed by thermal-gravimetric analysis that the carbonaceous species resulting from thermal decomposition of binder, plasticizer and PVA increase the final content of carbon in the multilayer after de-binding up to 5.4 wt%.

A final pressureless sintering treatment has been performed under argon atmosphere (pressure of 500–600 mbar) at 2170 °C for 30 min.

Two kinds of specimens were prepared for microstructure and mechanical characterization and for re-entry simulation tests, respectively. Flat plates 80 mm × 20 mm × 2 mm were prepared for re-entry tests, while flat bars 50 mm × 10 mm × 2 mm were processed for mechanical tests.

Table 1
Slurry and dry green tape compositions

Components		Composition (wt%)			
		Slurry type A	Slurry type B	Dry green tape A	Dry green tape B
Ceramic powder	SiC	28.0	33.6	58.7	67.7
Sintering aids	B	0.3	0.3	0.6	0.6
	C	0.8	1.0	1.7	2.0
Pore-forming agent	Starch	3.3	–	6.9	–
Solvents	Ethyl alcohol	12.2	11.8	–	–
	Buthanol	18.8	18.0	–	–
	Tetrachloroethylene	21.4	20.6	–	–
Dispersant	Fish oil	0.1	0.1	0.2	0.2
Binder	Polyvinylbutyral	5.2	5.0	10.9	10.1
Plasticizer	Polyethylenglycole	10.0	9.6	21.0	19.4

2.2. Material characterization

The size and the weight of the specimens were measured by using an electronic calliper and an electronic balance, respectively. The surface roughness was investigated using MAHR Perthometer M1 equipment. The microstructure of the samples was studied by X-ray radiography, X-ray diffraction, optical and scanning electron microscope (equipped with EDS analyser). Mercury intrusion porosimetry was used for investigating the open porosity. The thermal stability and oxidation resistance of the material was checked by submitting small specimens cut from the bars of multilayer SiC to DTA–TGA–MS simultaneous analysis both under argon and air flow. Three-point bending tests were performed adopting a distance between external rollers of 40 mm (UNI EN 658.3 standard), elastic modulus was measured by using a technique based on impulse excitation technique and analysis of transient natural vibration (GrindoSonic MK5 equipment, ASTM C 1259-01). Vickers microhardness measurements were performed on the crosssection of the specimens also with the aim of investigating crack propagation.

Size, density, surface roughness, open porosity, microstructure, stiffness and flexural strength were checked also for specimens that sustained many re-entry simulations. After the re-entry tests, bars with 80 mm × 10 mm × 2 mm were machined out of the centre of the test plates, representing the parts that had experienced the most severe thermal loads during re-entry cycles. By using these bars the mechanical properties after 100 re-entry simulations were checked. The three points bending test was performed using a 40 mm outer span in order to allow the comparison of these results with the corresponding ones obtained for the as-processed materials.

2.3. Re-entry simulation tests

The specimens of multilayer SiC were examined before the test in terms of weight, size and aspect; both front and back side of specimens were scanned by using a CanoScan LIDE 60 scanner. In order to avoid errors due to moisture, samples have been dried overnight at 130 °C/<20 mbar in a Heraeus-made vacuum dryer before measuring their weight.

Tests were performed in ARC's Re-Entry Simulation Chamber. Test conditions, i.e. thermal and atmospherical load profiles, were selected according to the HERMES study. These profiles have already been employed in the ESA study "OLCHOS" on OPS performance of C_f/SiC composites for re-usable heat shields.[13,14] Therefore, background data and experience in materials performance under these specific re-entry test conditions are available and allow a thorough interpretation of test results, including a comparison to the performance of most recent TPS concepts.

Two types of laminated multilayer silicon carbide plates (four specimens of kind "A" integrating one porous layer out of five and four specimens of kind "B" containing dense SiC layers only) were subject to thermal re-entry testing under OLCHOS type test conditions. Maximum temperatures were set to 1450 or 1550 °C. A maximum of 100 combined thermal and air pressure cycles were performed. Sample mass and sample aspect were recorded in regular intervals, i.e. after 1, 2, 5, 10, 20, 30, 50, 70, and 100 cycles, while microstructure and mechanical behaviour were investigated after 100 cycles. Details on the test conditions are presented in Fig. 1.

A modified test set-up has been applied for the vacuum testing of a further sample of type "B". The thermal profile with maximum temperature of 1550 °C has been selected, but at a vacuum <10^{-5} mbar.

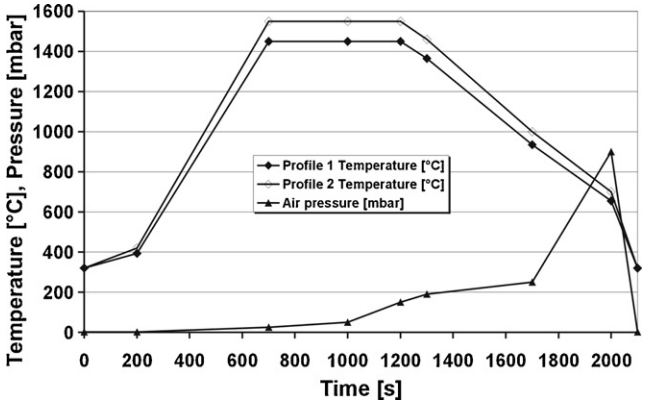

Fig. 1. Thermal and pressure profiles for re-entry testing.

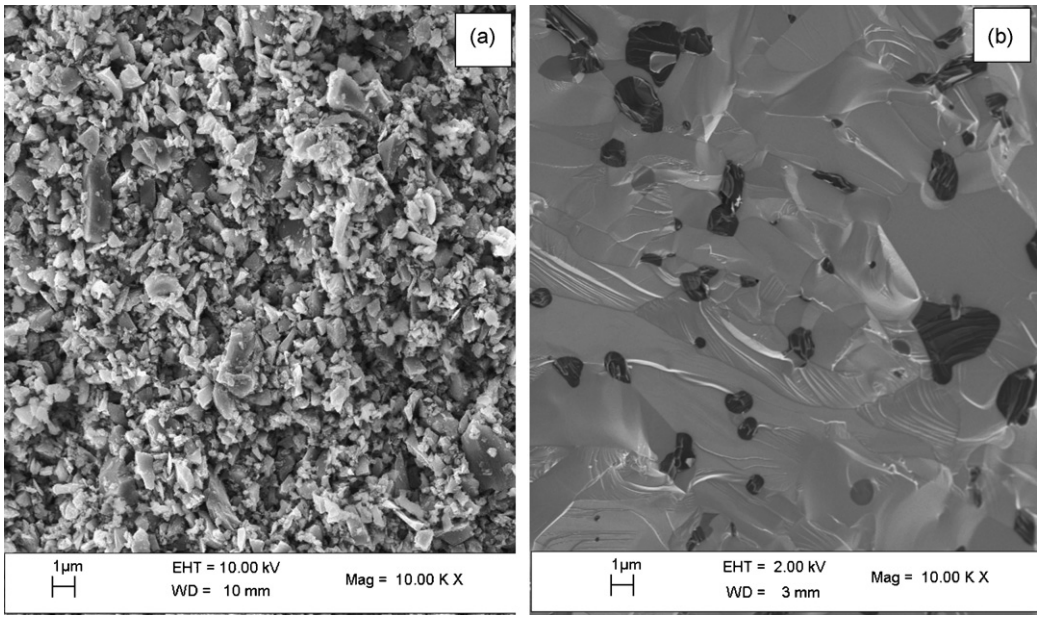

Fig. 2. Surface fracture of multilayer SiC after de-binding (a) and after sintering (b).

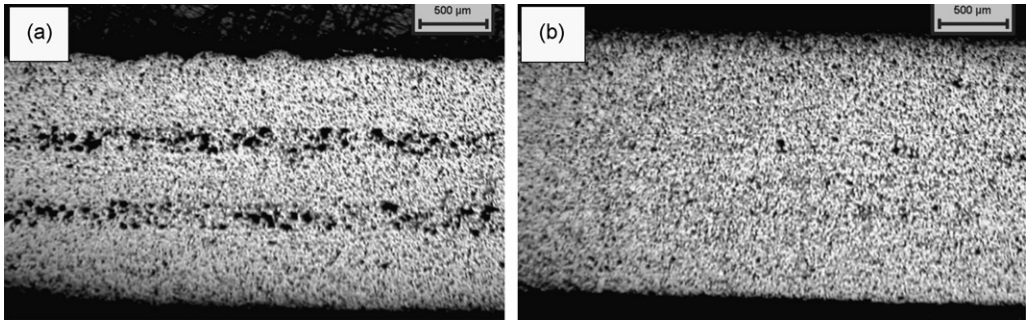

Fig. 3. Crosssection of multilayer SiC: integrating porous layers (a) and with dense layers only (b).

3. Results and discussion

3.1. Microstructure and physical characteristics of the as processed material

The multilayer SiC of type "B" shows extended porosity after de-binding that is almost completely eliminated after sintering up to 2170 °C; its microstructure is characterized by the presence of carbon particles inside the SiC layers, while the single layers are not clearly distinguishable after sintering (Figs. 2 and 3). On the contrary, in the case of multilayer SiC of type "A" starch decomposition leaves pores with large size after de-binding that are not completely recovered during sintering, thus porous layers can be are easily detected on the crosssection of the material owing to residual porosity (Fig. 3). In any case the interfacial bonds between the layers seem strong enough to avoid the formation of large voids or delamination surfaces that in fact were never detected by microscopy and X-ray radiography at these interfaces. On the other hand, some weakness of the interface between dense and porous layers has to be inferred in order to explain the crack deflection that has been observed to occur in this zone. Actually by Vickers indentation it is possible to cause the formation of cracks on the crosssection of the multilayer SiC and observe their propagation. Surprisingly, in any case four radial cracks do not form as usual, but only two cracks were observed that at the beginning run parallel to the laminate surface and then bend towards the surface. These cracks can be also deflected at the interfaces between porous and dense layers (Fig. 4). This peculiar behaviour probably is due to residual stresses and debonding at the interfaces between the layers.

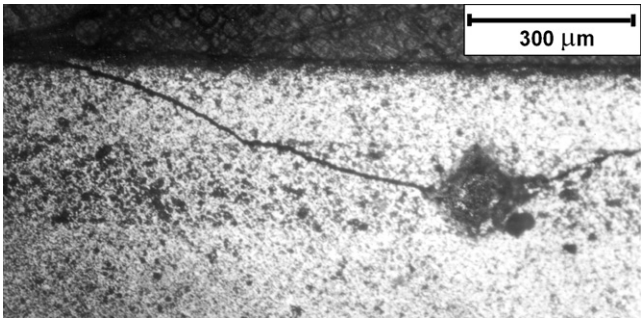

Fig. 4. Crack deflection at interfaces between adjacent layers.

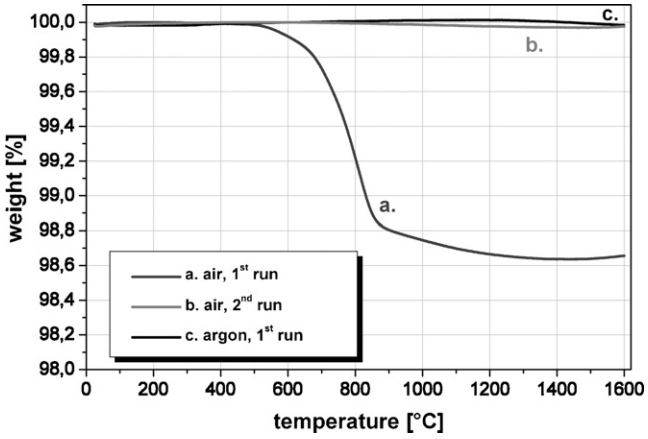

Fig. 5. TGA curves obtained for multilayer SiC under different conditions: first run under air flow (a), second run under air flow (b) and first run under argon flow (c).

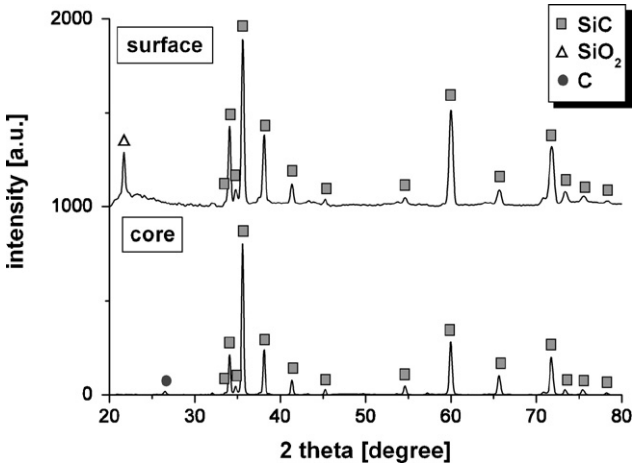

Fig. 6. XRD obtained after oxidation of a multilayer SiC integrating one porous layer out of two: comparison between the pattern recorded on the surface and that recorded on the crosssection at the core of the specimen.

The oxidation of multilayer SiC in air under atmospheric pressure at high temperature is dominated by two phenomena: the oxidation of carbon present on the surface (and resulting from the adoption of sintering aids as well as from the decomposition of some organic components of the slurry), and the subsequent oxidation of SiC allowing for self-passivating behaviour. In Fig. 5, three TGA curves are compared. These curves refer to weight changes occurring during: heating in air up to 1600 °C (Curve a), re-heating of the same specimens at the same conditions (Curve b), and heating of the as-processed material under argon atmosphere (Curve c). The weight change observation was combined with the results of the simultaneous analysis of the gaseous species flowing out from the TGA equipment cell by mass spectrometry. The first TGA run under air flow causes firstly a loss of weight owing to carbon combustion while a slight weight increase due to formation of a surface silica layer can be appreciated between 1400 and 1600 °C. The same sample does not suffer weight changes during a second run in air because of the protective effect of the surface oxide layer. When the material is heated under inert argon atmosphere, no relevant effect is observed owing to its high thermal stability. Self-passivating behaviour consisting in the formation of a crystalline silica layer was displayed also by multilayer SiC integrating many porous layers (up to 50% of porous layers), which lowers down the density to 83% of the theoretical one for SiC (Fig. 6). Fig. 7 shows the morphology of the oxide layer formed after 30 h at 1600 °C in air under atmospheric pressure. Previous investigations showed that oxidation in air under atmospheric pressure, resulting in the formation of the passivating surface layer, causes a decrease of strength, ranging between 20 and 40% of the original value and depending on the thickness of the single layers stacked in the multilayer architecture.[15] The mechanical features of the as-processed multilayer SiC under present investigation are reported in Table 2.

3.2. Material modifications detected during re-entry tests

All specimens showed a significant mass loss after the first thermal cycle. When testing at 1450 °C maximum temperature, this average mass loss was 1.84% for type "A" specimens with porous layers, and 1.40% for type "B" samples without porous layers. At the higher testing temperature of 1550 °C, these initial average mass losses amounted to 1.25% for type "A" laminate, and to 1.12% for type "B" one. Despite the high scattering and the limited number of specimen, it seems that the higher testing temperature results in a slightly lower mass change after the first

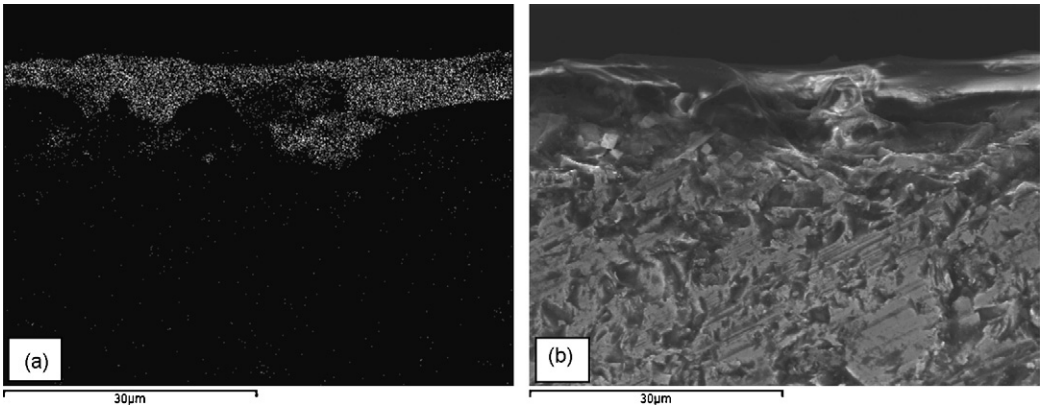

Fig. 7. Continuous surface silica layer grown after oxidation in air (30 h at 1600 °C): oxygen map (a) and crosssection microstructure (b).

Table 2
Comparison of physical properties of multilayer SiC of type "A" and "B" before and after 100 re-entry cycles

Specimen history		Young modulus (GPa)	Bending strength (MPa)	HV (kg/mm^2) (load 200 g)	Density variation (%)
Type "A"	Before re-entry test 358	304		2500[a] 1350[b]	–
	After 100 re-entry tests (T_{MAX} = 1450 °C)	131	114	250–600	−0.56
	After 100 re-entry tests (T_{MAX} = 1550 °C)	130	90	200–500	0.32
Type "B"	Before re-entry test	323	321	2500[c]	–
	After 100 re-entry tests (T_{MAX} = 1450 °C)	163	109	200–600	−1.25
	After 100 re-entry tests (T_{MAX} = 1550 °C)	160	101	200–500	−0.90
	After 100 re-entry tests (T_{MAX} = 1550 °C, under vacuum)	163	115	200–1500	−1.20

[a] Detected as average value on dense layers.
[b] Detected as average value on porous layers.
[c] With respect to fully dense SiC.

cycle. At any rate, during every cycle oxidation of SiC to silica also happens, that counterbalances the weight loss due to carbon combustion.

After the initial mass loss during the first thermal cycle due to carbon oxidation, all specimens gain mass due to the oxidation of SiC to SiO_2 according to the reaction scheme:

$$2SiC_{(s)} + 3O_{2(g)} \rightarrow 2SiO_{2(s)} + 2CO_{(g)} \quad (1)$$

The mass gain/mol is 50% (40.10 g/mol SiC and 60.08 g/mol SiO_2). From this, reaction kinetics could be determined, provided that the competing reaction under formation of volatile SiO does not take place. This was however not done due to the highly instationary test conditions, involving thermal cycling, thermal gradients over the sample length, and varying oxygen partial pressures.

According to thermochemical analysis[4] and temperature/pressure profiles adopted for re-entry tests in air (Fig. 1), conditions suitable for passive oxidation resulting in silica formation occur when heating (between 800 °C and maximum temperature) and when cooling (between maximum temperature and 800 °C) as well. On the contrary, during the beginning of the isothermal step at 1450 °C, transition to active oxidation should happen, when pressure is set at 25 mbar (but not for pressures of 50 and 150 mbar), according to the following reactions:

$$SiC_{(s)} + 2SiO_{2(s)} \rightarrow 3SiO_{(g)} + CO_{(g)} \quad (2)$$

$$SiC_{(s)} + SiO_{2(s)} \rightarrow 2SiO_{(g)} + C_{(s)} \quad (3)$$

$$2SiC_{(s)} + SiO_{2(s)} \rightarrow 3Si_{(l)} + 2CO_{(g)} \quad (4)$$

The first of these reactions should also occur when temperature is 1550 °C and pressure is 50 mbar (but not when P = 150 mbar).

Conclusively according to[4] the specimens are exposed to passive oxidation for about 20 or 23 min when cycled up to 1450 or 1550 °C, respectively; conditions suitable for active oxidation are sustained by the specimens during the same cycle for periods ranging between 5 and 8 min and depending on the maximum temperature. It shall however be mentioned that the actual transition between active and passive oxidation is strongly influenced by the structure of the SiC, the presence of contaminations, and the thickness and structure of a silica layer already formed.

Presenting the mass change in the usual way, i.e. relating the sample mass after a number of cycles to the sample's initial mass, results in graphs that are not easy to understand because of the high initial sample mass loss during the first cycle. Mean values of mass change as a function of cycle number is presented in Fig. 8.

These results indicate that the initial mass loss of most of the samples is in the same range as any subsequent mass gain during 100 thermal cycles. However, the mass gain observed after several cycles was found higher in the case of specimens integrating porous layers and it increased with the maximum temperature increase.

For type "A" multilayer SiC (with porous layers), the maximum mass loss is achieved after the first cycle when tested at 1450 °C, while samples tested at 1550 °C loose additionally about 0.1% of their initial mass until the 5th cycle. This subsequent mass loss is however very small compared to the initial mass loss of 1.2%.

It is remarkable that the initial mass loss is significantly higher for samples tested at 1450 °C compared to samples tested at 1550 °C. The reason may be that the mass gain from the oxidation reaction at the higher temperature of 1550 °C is

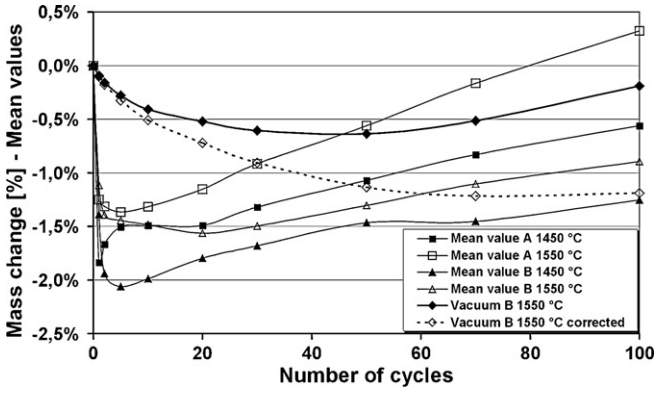

Fig. 8. Mass change of all samples (average of twin values for each material and cycling conditions) tested in air and comparison with mass change suffered by specimen tested under vacuum.

overruling some of the mass loss due to the oxidation of free carbon.

For type "B" multilayer SiC, the initial mass loss is also predominant, but even at subsequent thermal cycles, a mass loss is observed. At 1450 °C, the mass loss after the first cycle is around 1.4%, and after 5 cycles, this is increased to around 2%. The mass does however not change much between the second (1.9%) and the tenth (2.0%) cycle.

At 1550 °C, the mass loss is again smaller, and the highest mass loss is observed only after the 20th cycle, with about 1.6%. Again, the mass does not change much between the second (1.4%) and the 30th (1.5%) cycle. The "plateau" of almost constant mass is therefore much broader compared to tests at 1450 °C.

In order to explain the complex trend of the curves showing the mass change at least three main phenomena (namely carbon combustion, passive and active oxidation of SiC) should be considered. Furthermore, the test performed under high vacuum showed that also volatilization of SiC can happen to a certain extent.

The oxidation rate of the two types of laminates cannot be calculated from the existing data, as all tests were performed under instationary conditions, both in pressure and in temperature. Anyway, a graph similar to the commonly used Arrhenius plot reveals that the rate of the oxidation reaction is significantly higher for the type "A" samples rather than for the type "B" samples. This is presented in Fig. 9. For estimating the rate, only mass change after 50, 70, and 100 cycles has been regarded.

The reason for the higher reaction rate of specimens integrating porous layers (type "A") could be tentatively attributed to the exposition at the oxidising atmosphere of the layers with enhanced porosity in correspondence of the lateral sides of the specimens. Oxygen could diffuse more easily in a direction parallel to the stacked layers, preferentially penetrating inside the porous layers starting from the small lateral surfaces.

The material of type "B" has been tested under high vacuum to separate the oxidation and the possible evaporation terms of the mass changes observed within this study. The different behaviour of multilayer SiC of type "B" under high vacuum conditions is presented in Fig. 8. It is obvious that the mass loss in the first cycle is significantly lower when tests are preformed

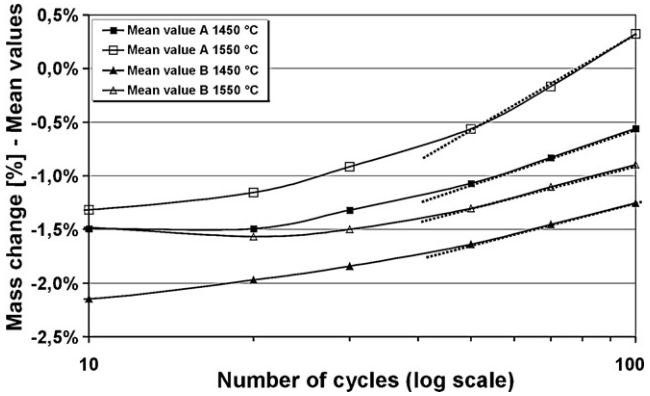

Fig. 9. Simplified Arrhenius-type plot and straight dotted lines for oxidation rate.

in absence of oxygen because carbon oxidation can not occur (unless it involves oxygen possibly contaminating the SiC raw powder), but there is an apparent subsequent mass gain of the sample tested under vacuum. This has to be attributed to platinum and rhodium deposition to the sample because of the high susceptor temperature in vacuum, causing in situ sputtering of the specimen. Actually these metals were detected on the surface of the specimen submitted to this test by using both SEM-EDS and micro-XRD. The overall sputter rate has been estimated with approximately 0.01 mass% for each cycle. With this estimation, an approximated "real" mass change of the sample tested under vacuum has been calculated. This is also presented in Fig. 8. It must however be mentioned that the estimated "sputter rate" is only valid for the vacuum tests, as testing under air results in different streaming conditions within the susceptor tube and a clearly lower Pt/Rh deposition on the samples.

After this correction the curve for mass change of the specimen tested under high vacuum shows a progressive mass loss with the number of cycles. The dominating degradation mechanism of SiC under vacuum seems volatilization of gaseous silicon, causing carbon enrichment and the deposition of solid carbon on the SiC surface. According to the literature[4] the tendency for SiC to undergo dissociation in vacuum should be irrelevant up to 1330 °C, since at these conditions the equilibrium pressure of gaseous silicon is negligible. On the other hand the present re-entry tests have been performed at higher temperature and under not stationary conditions (instead of equilibrium ones).

Tests under vacuum give some further indication, e.g. deposition of a glassy matter at the sample holder, which could be referred either to reaction of SiC with residual oxygen present in the test rig and oxygen that contaminated the specimens during sample preparation or to thermal decomposition of SiC.

3.3. Microstructure and physical characteristics of specimens after 100 re-entry cycles

After completing 100 cycles, all samples were intact, and no distortion or delamination has been observed, neither by visual inspection, X-ray radiography and size measurements. The surface roughness of specimens cycled at the maximum temperature of 1450 °C was similar to that of the as-processed material (3 μm) while increased roughness (6 μm) was observed for specimens cycled up to 1550 °C. In both cases crystals of silica protruding forward from the surface were observed after re-entry tests. The curves of pore size distribution before and after re-entry simulation, detected by mercury intrusion technique, are compared in Fig. 10. Open porosity sharply increases after re-entry tests, in addition the pore size distribution curves show that the size of open pores increases in the case of specimens tested either in oxidising environment or under vacuum. The crosssection of specimens shows a thin surface layer mainly constituted by silica, but containing also SiC as showed by elemental EDS maps (Fig. 11). X-ray diffraction patterns do not help to assess if the surface layer can be considered as a continuous layer ensuring protection against oxidation or not; in fact the intensity of peaks belonging to SiC decreases when

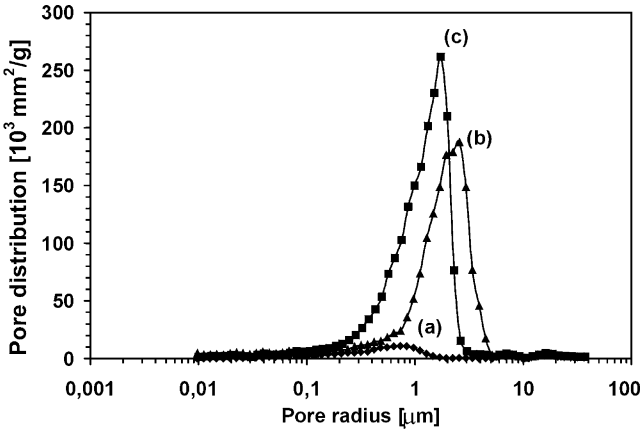

Fig. 10. Size distribution of open pores: as-processed material (a), after 100 cycles up to 1550 °C in air (b) and after 100 cycles up to 1550 °C under vacuum (c).

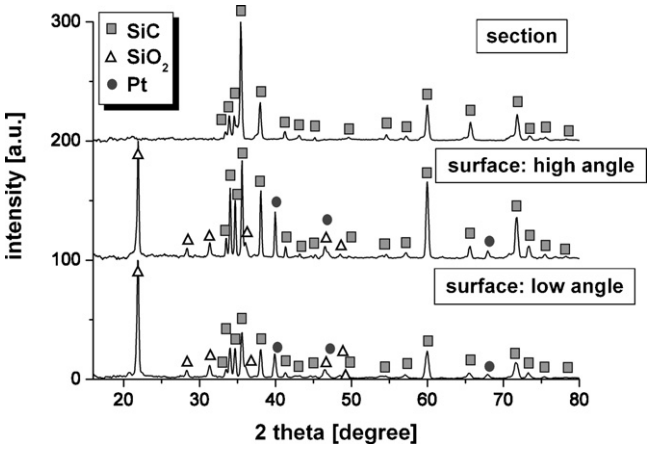

Fig. 12. XRD after re-entry tests (maximum temperature 1550 °C) of surface and crosssection of specimens.

low-angle diffraction is carried out but they do not disappear in the relevant X-ray pattern (Fig. 12). Nevertheless, oxygen concentration maps obtained on the transverse section of these specimens showed the presence of oxygen at the sample core and other degradation phenomena like formation of quite large voids and (only in few cases) of cracks (Fig. 13a and b). Moreover, from SEM-EDS analyses, oxygen seems to be distributed, within the crosssection, in the same way for type "A" specimens with porous layers and for type "B" samples without porous layers.

Owing to the porosity increase the hardness greatly decreases after re-entry tests, and it was found to vary in a wide range of values depending on the position where the Vickers indentation is performed (Table 2). X-ray diffraction technique was used to check the presence of residual stresses that in principle could rise during re-entry tests owing to thermal cycling. XRD did not give any evidence of important residual stresses, probably because they can be relieved by the formation of novel pores.

The microstructure (Fig. 13c) of the specimen submitted to 100 re-entry cycles under vacuum shows the same porosity

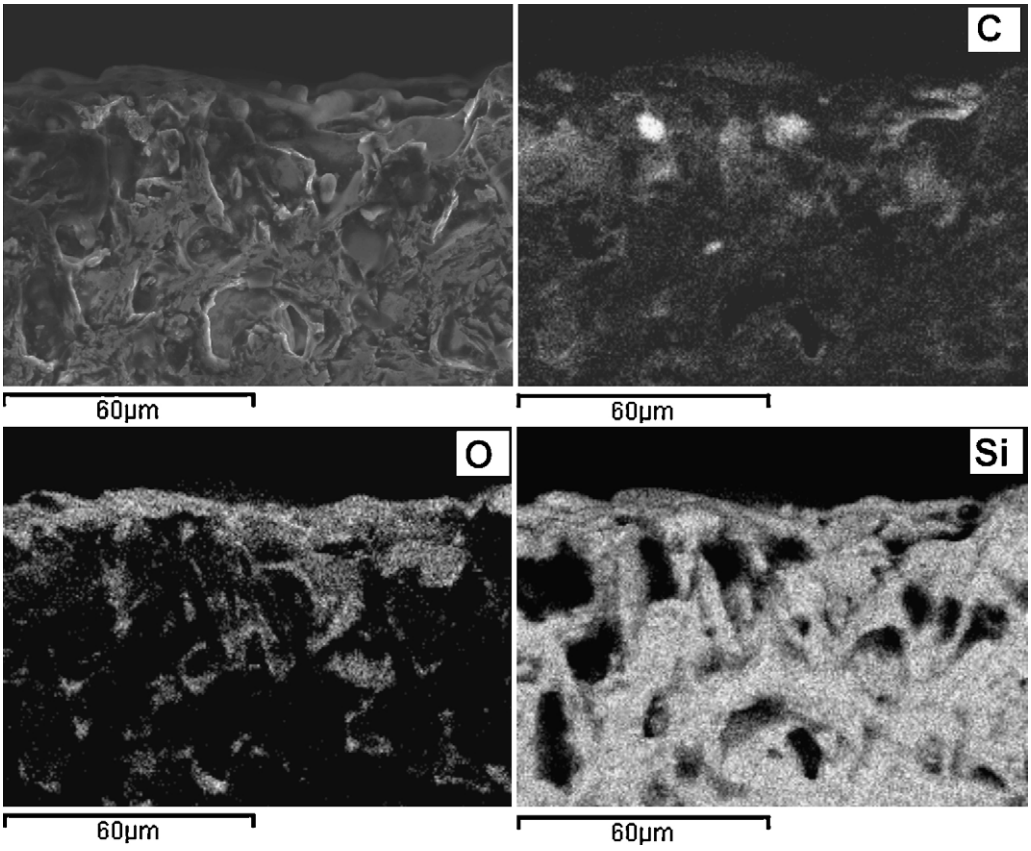

Fig. 11. Crosssection of specimens after re-entry tests: oxide layer grown on sample surface and elemental EDS maps.

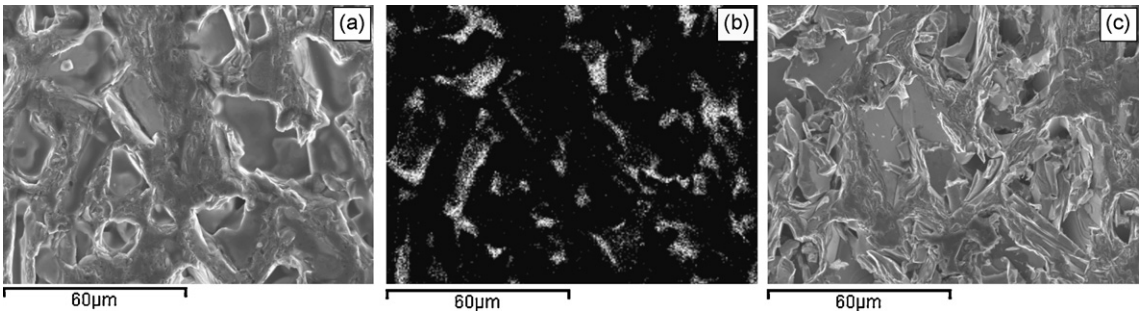

Fig. 13. Microstructure (a) and oxygen EDS map (b) at the core of specimens after 100 re-entry tests in air; microstructure after 100 re-entry tests performed under vacuum (c).

degree as observed for samples tested in oxidising environment. EDS analysis performed on a wide area on the section of specimens proved that the C/Si atomic ratio (about 1.18 for the as-processed material) increases up to up to 2.2 after 100 re-entry cycles under vacuum. Moreover, in the X-ray diffraction pattern of transverse section of specimen tested under vacuum the peak belonging to graphite appears, while it is present neither in the corresponding pattern of the samples tested in oxidising conditions nor in that of the as-processed multilayer. Even though silicon volatilization and deposition of solid carbon could also happen for specimens tested in air, the carbonaceous residue is then expected to be quickly depleted by reaction with oxygen.

Then the decomposition of SiC seems to be the main reaction responsible for the formation of porosity during testing under vacuum, and this may also concur with the active oxidation to cause degradation during testing in oxidising environment.

Surprisingly the bending strength and modulus after 100 re-entry simulations were found to be very similar for all the specimens of type "B", irrespective of the different experimental conditions that they experienced (maximum temperature, oxidising atmosphere or high vacuum). In order to separate the contributions to material degradation of active oxidation and silicon volatilization, further specimens protected from oxidation by a suitable surface coating or carrying a pre-formed thick and continuous passivating silica layer, should be investigated.

Anyway it is noteworthy that, whatever degradation mechanism could prevail, multilayer SiC proved to be a promising candidate for re-usable thermal protection systems, since bending strength as high as 100 MPa and elastic modulus over 130 GPa were measured for the material even after 100 re-entry simulation tests.

4. Summary and conclusions

Two kinds of multilayer SiC, processed by tape casting, debinding and sintering, were submitted to 100 re-entry tests in air under conditions similar to a HERMES trajectory (maximum temperature of either 1450 or 1550 °C), or under vacuum (maximum temperature 1550 °C).

These two kinds of laminates – one containing dense SiC layers only and the other one integrating some porous layers in the multilayer architecture – behaved in the same manner during testing in oxidising environment. During the few initial re-entry cycles carbon (added as sintering aid or left by thermal decomposition of the binder and plasticizer used for tape casting) burnt down. This phenomenon caused mass loss that was soon overruled by oxidation of SiC resulting in both silica formation and weight increase.

Due to the instationary test conditions, involving thermal cycling, thermal gradients over the sample length and changing oxygen partial pressure, the specimens could alternatively have experienced passive and active oxidation of SiC during every cycle. The occurrence of active oxidation could then have prevented the formation on the sample surface of a thick and continuous passivating silica layer, which normally grows under atmospheric pressure instead. For this reason also oxidation at the sample core happened to a certain extent.

In spite of these degradation phenomena all specimens did not suffer distortion or delamination and looked as intact after 100 re-entry simulations. On the other hand their microstructure appreciably changed owing to the formation of a silica layer on the surface and the increase of porosity at the sample core. The formation of novel porosity and the pore coalescence resulted in the significant decrease of hardness, flexural strength, and elastic modulus.

Also the multilayer SiC tested under high vacuum showed similar microstructure variation and degradation of mechanical behaviour. In this last case degradation can be attributed to thermal decomposition under vacuum of SiC, which results in the volatilization of silicon and the deposition of solid carbon within the SiC matrix. Owing to the emission of gaseous silicon a mass loss, increasing with the number of cycles, has been observed. This further degradation mechanism could occur also when testing is performed in oxidising environment and the pressure is reduced to few mbar. In order to distinguish the contribution of the different degradation mechanisms, and to slow down the material degradation as well, specimens completely protected against oxidation should be investigated. To this purpose, suitable surface coatings able to prevent oxidation or at least a pre-oxidation treatment of multilayer SiC, resulting in a thick surface layer displaying a passivating effect, could be adopted. Investigations on these topics are in progress.

Anyway, all the specimens after 100 re-entry simulations performed under different conditions (maximum temperature, oxidising atmosphere or vacuum) showed flexural strength of about 100 MPa and modulus over 130 GPa. Then multilayer SiC

can be regarded as a very promising material for application in re-usable thermal protection systems of re-entry space vehicles.

Acknowledgements

This work has been performed within the framework of the Integrated European Project "ExtreMat" (contract NMP-CT-2004-500253) with financial support of the European Community. It only reflects the view of the authors and the European Community is not liable for any use of the information contained therein.

References

1. Leiser, D. B., Space shuttle thermal protection system. *Am. Ceram. Soc. Bull.*, 2004, **83**(8), 44–47.
2. Wilson, A., ed., *Proceedings of the 4th European Workshop on "Hot Structure and Thermal Protection Systems for Space Vehicles"*. ESA-ESTEC, Noordwijk (The Netherlands), 2003, ISBN 92-9092-831-X.
3. Munro, R. G., Material properties of a sintered α-SiC. *J. Phys. Chem. Ref. Data*, 1997, **26**(5), 1195–1203.
4. Gulbransen, E. A. and Jansson, S. A., The high-temperature oxidation, reduction, and volatilization reactions of silicon and silicon carbide. *Oxid. Met.*, 1972, **4**(2), 181–201.
5. Jacobson, N. S., Fox, D. S. and Opila, E. J., High temperature oxidation of ceramic matrix composites. *Pure Appl. Chem.*, 1998, **70**(2), 493–500.
6. Clegg, W. J., The fabrication and failure of laminar ceramic composites. *Acta Metall. Mater.*, 1992, **40**(11), 3085–3093.
7. Zhang, J. X., Jiang, D. L., Qin, Sh. Y. and Huang, Zh. R., Fracture behaviour if laminated SiC composites. *Ceram. Int.*, 2004, **30**, 697–703.
8. Huang, R., Gu, H., Zhang, J. and Jiang, D., Effect of Y_2O_3–Al_2O_3 ratio on the inter-granular phases and films in tape-casting α-SiC with high toughness. *Acta Mater.*, 2005, **53**, 2521–2529.
9. Blanks, K. S., Kristoffersson, A., Carlstrom, E. and Clegg, W. J., Crack deflection in ceramic laminates using porous interlayers. *J. Eur. Ceram. Soc.*, 1998, **18**, 1945–1951.
10. Zhang, J., Huang, R., Gu, H., Jiang, D., Lin, Q. and Huang, Z., High toughness in laminated SiC ceramics from aqueous tape casting. *Scripta Mater.*, 2005, **52**, 381–385.
11. Stavrinidis, C., Tumino, G., Caporicci, M., Pradier, A., European technology development efforts in the field of structures in preparation of future reusable space transportation systems In Proceedings of the 1st AIAA/IAF Symposium on Future Reusable Launch Vehicles, 2002, 1830.
12. Biamino, S., Antonini, A., Pavese, M., Fino, P. and Badini, C., $MoSi_2$ laminate processed by tape casting: microstructure and mechanical properties' investigation. *Intermetallics*, in press.
13. In *Proceedings of the 1st AIAA/IAF Symposium on Future Reusable Launch Vehicles*, 2002.
14. Liedtke, V., Huertas Olivares, I., Langer, M. and Haruvy, Y. F., Manufacturing and performance testing of sol/gel based oxidation protection systems for re-usable space vehicles. *J. Eur. Ceram. Soc.*, 2007, **27**, 1493–1502.
15. Pavese, M., Fino, P., Ortona, A. and Badini, C., Potential of SiC multilater ceramics for high temperature applications in oxidising environment. *Ceram. Int.*, 2008, **34**, 197–203.